

Operational Monitoring of Weather Radar Receiving Chain Using the Sun

IWAN HOLLEMAN

Royal Netherlands Meteorological Institute (KNMI), De Bilt, Netherlands

ASKO HUUSKONEN AND MIKKO KURRI

Finnish Meteorological Institute, Helsinki, Finland

HANS BEEKHUIS

Royal Netherlands Meteorological Institute (KNMI), De Bilt, Netherlands

(Manuscript received 28 August 2008, in final form 10 August 2009)

ABSTRACT

A method for operational monitoring of a weather radar receiving chain, including the antenna gain and the receiver, is presented. The “online” method is entirely based on the analysis of sun signals in the polar volume data produced during operational scanning of weather radars. The method is an extension of that for determining the weather radar antenna pointing at low elevations using sun signals, and it is suited for routine application.

The solar flux from the online method agrees very well with that obtained from “offline” sun tracking experiments at two weather radar sites. Furthermore, the retrieved sun flux is compared with data from the Dominion Radio Astrophysical Observatory (DRAO) in Canada. Small biases in the sun flux data from the Dutch and Finnish radars (between -0.93 and $+0.47$ dB) are found. The low standard deviations of these sun flux data against those from DRAO (0.14 – 0.20 dB) demonstrate the stability of the weather radar receiving chains and of the sun-based online monitoring.

Results from a daily analysis of the sun signals in online radar data can be used for monitoring the alignment of the radar antenna and the stability of the radar receiver system. By comparison with the observations from a sun flux monitoring station, even the calibration of the receiving chain can be checked. The method presented in this paper has great potential for routine monitoring of weather radars in national and international networks.

1. Introduction

Whiton et al. (1976) first proposed the calibration of weather radar systems using the sun as a radio source. They describe how the sun signals can be used to determine the antenna orientation, the beam boresighting (difference between the normal to antenna aperture and beam direction), and the effective system gain (including one-way receiver losses). They concluded that the elevation and effective antenna system gain could be determined within 0.2° and 1.3 dB, respectively. Nowadays, the sun is commonly used for alignment of the

radar antenna, checking of antenna gain, and monitoring of the receiver calibration (Rinehart 2004). Offline sun measurements, in which the operational scanning of the radar is interrupted and the antenna is pointed at the sun, are routinely used for this.

Checking of weather radar systems using solar artifacts detected by operationally scanning radars (“online”) was first attempted by Andersson (2000). He showed that the sun signals found in operational scan data can be used for several health checks of a weather radar (e.g., the horizontal and vertical alignment of the antenna and the intensity measurements). Darlington et al. (2003) showed that sun signals can be detected automatically in polar scan data at long ranges and that the antenna azimuth bias can be determined with 0.1° precision. A method for online monitoring of the antenna pointing and the radar sensitivity using sun signals

Corresponding author address: Iwan Holleman, Royal Netherlands Meteorological Institute, P.O. Box 201, NL-3730 AE De Bilt, Netherlands.
E-mail: i.holleman@science.ru.nl

was developed by Holleman and Beekhuis (2004). The online sun monitoring method enables a daily health check of operational weather radars and can also be applied to archived volume data, whereas offline sun checks are only performed during radar maintenance. Huuskonen and Holleman (2007) presented the use of signals detected from the sun at low antenna elevations for determining the weather radar antenna pointing (i.e., the biases in elevation and azimuth). In addition, the impact of atmospheric refraction and attenuation was shown, and improved correction methods were presented.

In the present paper, we extend the sun-signal method to online monitoring of the weather radar receiving chain, including the antenna gain and the receiver, on a daily basis. The solar flux observed by the weather radars can be applied to monitor the stability of the receiving chain, the relative sensitivity of systems within national and international radar networks, and the calibration of the receiving chain. The conversion of the radar reflectivity from operational scan data to received solar flux at the top of the atmosphere is presented, and a validation against offline sun flux observations is made. Finally, results of successful routine application on the Dutch and Finnish weather radar networks are presented. For a detailed understanding of the online sun monitoring method, it is recommended to read our previous paper (Huuskonen and Holleman 2007) as well.

2. Method

a. Solar spectral power at antenna feed

The automated detection of sun signatures in polar volume data from scanning weather radars is described in Huuskonen and Holleman (2007). Basically, a consistent reflectivity signal (i.e., signal from a continuous radio-frequency source) at long ranges (>100 km) is searched along radials in the operational scan data. Data below 1° elevation are discarded to avoid severe refraction and to ensure that the long-range observations are above precipitation areas. Unfiltered reflectivity data are used for this analysis, because (time domain) Doppler clutter filters can attenuate the solar signal by several decibels. Depending on the hardware of the radar, the volume coverage pattern, the season, and the latitude of the radar, several tens of sun hits are found per day. A radar signal processor usually corrects the received echoes for background noise and for the range-dependent attenuation. The received solar spectral power at the antenna feed P_f (per MHz in dBm) can be calculated from the reflectivity signature as a function of range $Z(r)$ (in dBZ) using

$$P_f = Z(r) - 20 \log_{10} r - 2ar - C_r - 10 \log_{10} \Delta f, \quad (1)$$

where C_r is the radar constant in dB, according to Probert-Jones (1962); a is the one-way gaseous attenuation in dB km⁻¹; and Δf is the equivalent noise bandwidth in MHz (usually approximated by 3-dB bandwidth). The mean solar power \bar{P}_f , averaged over range, is stored with its elevation, azimuth, date, and timestamp (accuracy better than 10 s).

b. Atmospheric gaseous attenuation

The received solar spectral power has to be corrected for the gaseous attenuation in the atmosphere. Huuskonen and Holleman (2007) have shown that this attenuation A_{gas} as a function of the solar elevation el_{sun} can be approximated by

$$A_{\text{gas}}(\text{el}_{\text{sun}}) \approx a \cdot \left(R_{43} \sqrt{\sin^2 \text{el}_{\text{sun}} + \frac{2z_0}{R_{43}}} - R_{43} \sin \text{el}_{\text{sun}} \right), \quad (2)$$

where R_{43} is the $4/3$ radius of the earth (Doviak and Zrnic 1993) and a is the one-way gaseous attenuation at ground level (0.008 dB km⁻¹ at C band). The equivalent height z_0 of the atmosphere is chosen such that the integrated density is conserved,

$$z_0 = \frac{RT_0}{g}, \quad (3)$$

where T_0 represents the atmospheric temperature at ground level, R is the gas constant, and g is the gravitation constant. The attenuation is calculated with a constant equivalent height of 8.4 km obtained using the surface temperature from the *U.S. Standard Atmosphere, 1976* ($T_0 = 288.15$ K). For elevations below 5°, the attenuation is rapidly increasing to over 2 dB for C-band radars. Huuskonen and Holleman (2007) have validated Eq. (2) by analyzing the sun hits per elevation and found good agreement with observations. The mean received solar spectral power at the antenna feed is corrected for this attenuation using

$$P_s = \bar{P}_f + A_{\text{gas}}(\text{el}_{\text{sun}}). \quad (4)$$

c. Modeling of sun hits

All solar signatures detected per day are analyzed using the linear model and fitting procedure described extensively in Huuskonen and Holleman (2007). For convenience, a short summary is provided here. The received solar power as a function of the radial distance to the

antenna beam axis is approximated by a Gaussian, and thus the power P_s (per MHz in dBm) can be written as

$$P_s(x, y) \equiv a_x x^2 + a_y y^2 + b_x x + b_y y + c, \quad (5)$$

where the coordinates in azimuth x and elevation y are defined as

$$x = az_{\text{read}} - az_{\text{sun}} \quad \text{and} \quad (6)$$

$$y = el_{\text{read}} - el_{\text{sun}}, \quad (7)$$

where ‘‘read’’ refers to the angle reading of the radar antenna. Equation (5) is linear in the parameters a_x to c ; thus, the sun data can easily be fitted to this equation by the least squares method. Parameters a_x and a_y can be estimated from the antenna beamwidth, and they are kept constant during the fit to increase the fit stability (Huuskonen and Holleman 2007). The elevation and azimuth biases of the radar antenna can be calculated from b_x and b_y , but they are not discussed here. From the parameters, the peak solar power P_0 (per MHz in dBm), that is, when radar antenna and sun are perfectly aligned, can be obtained using

$$P_0 = c - \frac{b_x^2}{4a_x} - \frac{b_y^2}{4a_y}. \quad (8)$$

Sometimes the sun signatures are contaminated by precipitation or radio-frequency interference (RFI) signals and therefore the deviations of the sun signatures from the first fit are determined. Outliers (i.e., observed sun power exceeding the fit model by 3 dB, about five standard deviations) are removed from the dataset prior to a second fit. From this second fit, the final estimate of the peak solar power P_0 is obtained. The standard deviation of the estimated peak solar power, calculated during the fit from the chi-square residual (Press et al. 1992), serves as a sensitive quality measure of the daily analysis.

d. Antenna beamwidth and scanning losses

The observed solar spectral power is attenuated by the imperfect overlap with radar antenna beam pattern and the averaging of received power while the radar antenna is scanning in azimuth. Assuming a uniform disk for the sun and a Gaussian antenna gain pattern, the solar power S as a function of the radial distance from the center ρ and the antenna gain G as a function of the radial distance from the center q can be parameterized by

$$S(\rho) = \begin{cases} \frac{4}{\pi \Delta_s^2} & \text{if } \rho < \frac{\Delta_s}{2} \\ 0 & \text{else} \end{cases} \quad \text{and} \quad (9)$$

$$G(q) = \exp\left(\frac{-4 \ln 2 q^2}{\Delta_r^2}\right), \quad (10)$$

where Δ_s and Δ_r are the apparent diameter of the radio sun (0.57°) and the 3-dB beamwidth of the radar antenna, respectively, and S and G are normalized such that the integrated solar power and the maximum gain of the radar antenna are equal to one. When the centers of the sun and the antenna are misaligned by x (azimuthal deviation), ρ and q are related by

$$q^2 = \rho^2 + x^2 - 2\rho x \cos \phi, \quad (11)$$

where ϕ represents the angle of the polar coordinate system for integration over the solar disk. The transmission loss $L(x)$ of the solar power received by an antenna pointing in elevation at the sun ($y = 0$) can then be calculated from

$$L(x) \equiv \int_0^\infty \int_0^{2\pi} G(q)S(\rho)\rho \, d\phi \, d\rho \approx L_0 \exp\left(-\frac{4 \ln 2 x^2}{\Delta_r^2}\right), \quad (12)$$

where L_0 is defined as

$$L_0 \equiv \frac{\Delta_r^2}{\ln 2 \Delta_s^2} \left[1 - \exp\left(-\frac{\ln 2 \Delta_s^2}{\Delta_r^2}\right) \right]. \quad (13)$$

The integral of the exponent-cosine term over ϕ is neglected, because it is one in first order. When the radar antenna is pointing at the sun ($x = 0$), the beamwidth correction is given by L_0 in agreement with Tapping (2001).

For a radar antenna pointing in elevation at the sun and scanning in azimuth through the sun, the mean transmission loss L_a can be calculated by integrating $L(x)$ from Eq. (12):

$$L_a \equiv \frac{1}{\Delta_a} \int_{-\Delta_a/2}^{\Delta_a/2} L(x) \, dx = L_0 \sqrt{\frac{\pi \Delta_r^2}{4 \ln 2 \Delta_a^2}} \operatorname{erf}\left(\frac{\sqrt{\ln 2} \Delta_a}{\Delta_r}\right), \quad (14)$$

where Δ_a is the angle over which the echoes are integrated to produce a ray and ‘‘erf’’ refers to the error function (Press et al. 1992). The calculated total correction for beamwidth and scanning losses as a function of the beamwidth of the radar antenna Δ_r is displayed in Fig. 1, which shows curves for different ratios of the processing width Δ_a and the antenna beamwidth. The solid line in the figure ($\Delta_a = 0$) shows the beamwidth correction for a radar antenna pointing statically at the

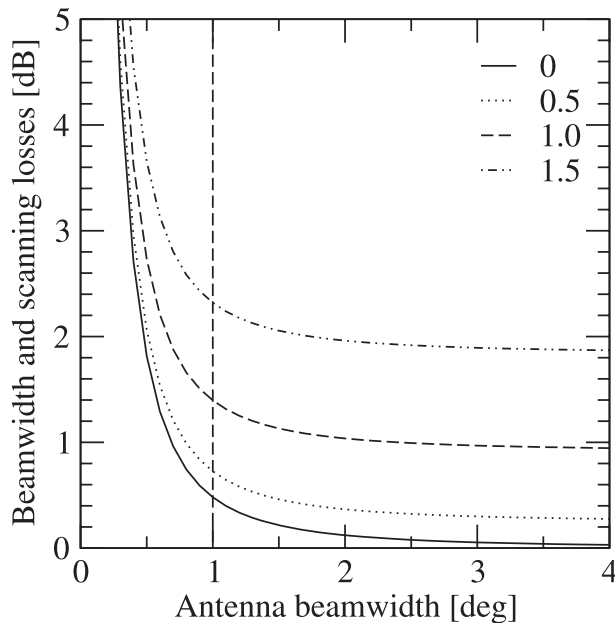


FIG. 1. The calculated correction for the beamwidth and the scanning losses as a function of the 3-dB width of the radar antenna Δ_r . Curves for different ratios (0–1.5) of the azimuthal averaging width Δ_a and the 3-dB antenna beamwidth are shown. The solid curve (0) is valid for a radar antenna pointing statically at the sun.

sun. It is evident that for antenna beam widths below 1° the losses are increasing rapidly. Furthermore, it is seen that the scanning of the antenna introduces substantial (typically about 1 dB) additional losses, because a scanning antenna simply cannot point optimally at the sun all of the time.

e. Conversion to solar flux

For operational monitoring of the radar sensitivity, all sun hits are collected, corrected for attenuation, and analyzed on a daily basis using the model described previously. To facilitate monitoring of radars in an

international or national network, the peak solar power is converted to solar flux F_s using

$$F_s = \frac{2 \times 10^{13} P_0}{L_a A_e}, \quad (15)$$

where F_s is given in solar flux units (sfu; $10^{-22} \text{ W m}^{-2} \text{ Hz}^{-1}$) and P_0 is the estimated peak solar power in mW MHz^{-1} . The factor 2 is added to correct for the single-polarization reception by the radar receiver of the unpolarized solar radiation. The effective antenna area A_e in m^2 is calculated from (Probert-Jones 1962)

$$A_e \equiv \frac{\lambda^2 G}{4\pi}, \quad (16)$$

where λ and G refer to the radar wavelength in meters and the antenna gain in linear units, respectively.

3. Available data

a. KNMI radar network

Since 1997, the Royal Netherlands Meteorological institute (KNMI) maintains an operational network of two identical C-band Doppler weather radars. One radar is located at KNMI in De Bilt (52.10°N , 5.18°E), and the other one is located at a naval air base in Den Helder (52.96°N , 4.79°E). The relevant technical parameters are given in Table 1. Every 5 min, the radars perform a 14-elevation volume scan between 0.3° and 25° elevation and only the lowest elevation is scanned in long-pulse mode. The pulse repetition frequency (PRF) increases from 250 Hz (single PRF) at the lowest elevation to 900/1200 Hz (dual PRF; see, e.g., Sirmans et al. 1976; Holleman and Beekhuis 2003) at the highest elevations. At the same time, the rotation velocity of the antenna increases from 15° to 36° s^{-1} . Polar volume data with

TABLE 1. Listing of relevant technical parameters of selected Doppler weather radars involved in this study. Note that the last four rows list the values for short- and long-pulse modes.

Parameter	De Bilt	Luosto
Manufacturer	SELEX-SI	SELEX-SI/Sigmat
Radar system/processor	Meteor 360AC/GDRX	Meteor 500C/RVP7
Geographical position	52.10°N , 5.18°E	67.13°N , 26.90°E
Wavelength	5.33 cm	5.33 cm
Polarization	Horizontal	Horizontal
Antenna gain	45.4 dBi	47.5 dBi
Beamwidth	0.94°	0.70°
Pulse duration	0.84/2.0 μs	0.9/1.9 μs
Noise level	$-112/-116$ dBm	$-107/-110$ dBm
Receiver bandwidth	1.5/0.6 MHz	1.5/0.6 MHz
Radar constant	66.21/62.91 dB	65.76/62.03 dB
Transmitted peak power	280/240 kW	260/260 kW

(unfiltered) reflectivity, mean radial velocity, and spectral width are produced and archived. More details are provided in Beekhuis and Holleman (2008).

b. FMI radar network

The Finnish Meteorological institute (FMI) operates a network of eight C-band Doppler weather radars. The Luosto radar (see Table 1) has a 6-m-diameter antenna and hence a beamwidth of about 0.7° . The other radars have a smaller antenna and a beamwidth just below 1° . Every 15 min, the radars perform an 11-elevation volume scan between 0.3° and 45° elevation, where six elevations up to 9° are scanned in long-pulse mode. At every 5 min, five of these six elevations are repeated. Polar volume data with (unfiltered) reflectivity, mean radial velocity, and spectral width are produced and stored. More details are given by Salonen et al. (2008).

c. DRAO sun observatory

The solar flux at a wavelength of 10.7 cm (S band) is continuously monitored at the Dominion Radio Astrophysical Observatory (DRAO; available online at <http://www.drao.nrc.ca>) in Canada. This observatory is located at a site near Penticton, British Columbia, which enjoys extremely low interference levels at centimeter wavelengths (Tapping 2001). Observations of the daily solar flux have started in 1946 and have continued to the present day. The current solar flux at 10.7 cm can be obtained from the Web site of the DRAO observatory and is updated each day at 2300 UTC. The solar flux values are corrected for the atmospheric attenuation.

The $F_{10.7}$ solar flux measurements can be converted to other radio frequencies with an accuracy of roughly 1 dB (Tapping 2001). This is possible, because the solar emission at centimeter wavelengths can be divided into two distinct components: a steady base level and a superimposed slowly varying component with a constant spectral shape. The estimated solar flux at C band (F_5) is

$$F_5 = 0.71(F_{10.7} - 64) + 126, \quad (17)$$

where the fluxes are given in sfu.

4. Online and offline results

a. Daily online analysis

Figure 2 presents the daily analysis of the sun signals detected in the operational scan data from the KNMI weather radars in De Bilt and Den Helder. Results are shown from 1 January to 15 February 2008 and unfiltered reflectivity data are used. Figure 2 (bottom) shows the number of analyzed sun signatures per day,

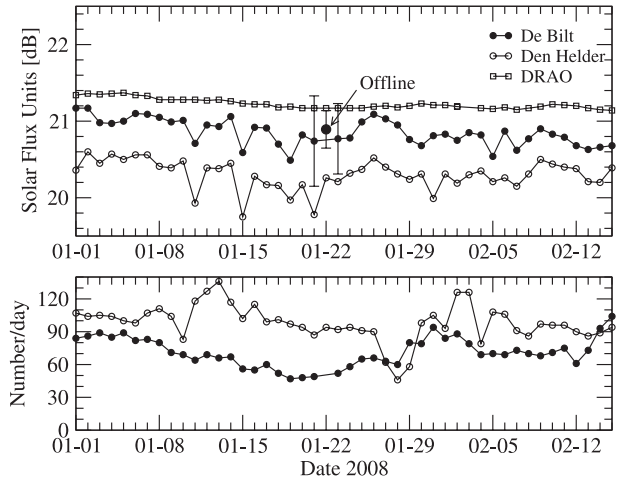


FIG. 2. Daily analysis of the sun signatures observed by the weather radars in De Bilt (filled circles) and Den Helder (open circles) from 1 Jan to 15 Feb 2008. For reference the observations from DRAO extrapolated to C band are plotted as well. (top) The solar flux and (bottom) the number of analyzed sun signatures per day are shown. The result from the offline sun tracking in De Bilt on 22 Jan 2008 is also plotted. The error bars indicate the std devs of the offline and online (2 days only) sun flux data.

and Fig. 2 (top) shows the deduced solar flux in sfu on a decibel scale. The standard deviations of the daily sun fluxes (only shown for two days in the figure) are calculated from the chi-square residual of the fit and vary between roughly 0.4 and 0.6 dB during this period. When the daily solar flux data from the De Bilt radar are referenced against those from the Den Helder radar, a bias of +0.54 dB and a standard deviation of 0.14 dB are found for this period. Thus, it is concluded that the receiver sensitivity of the two KNMI weather radars agrees within roughly half a decibel.

The daily solar flux as observed by the DRAO and extrapolated to C band using Eq. (17) is also plotted in Fig. 2. The daily sun flux observed by the weather radar in De Bilt is somewhat below the DRAO reference; for Den Helder, a larger underestimation is seen. The receiving bias of De Bilt with respect to DRAO is -0.38 dB, and the standard deviation of the daily ratios is only 0.14 dB for the 45-day period shown in the figure. For Den Helder, a receiving bias of -0.93 dB and a standard deviation of 0.17 dB are obtained for the same period. Note that the daily standard deviation of the DRAO flux data, calculated against a 7-day running average, is only 0.02 dB.

Figure 3 presents corresponding results from the FMI weather radars in Vimpeli (63.10°N , 23.82°E) and Luosto from 1 July to 13 August 2008. The lower number of sun hits in the FMI data is due to the smaller number of elevation angles used in the analysis. FMI

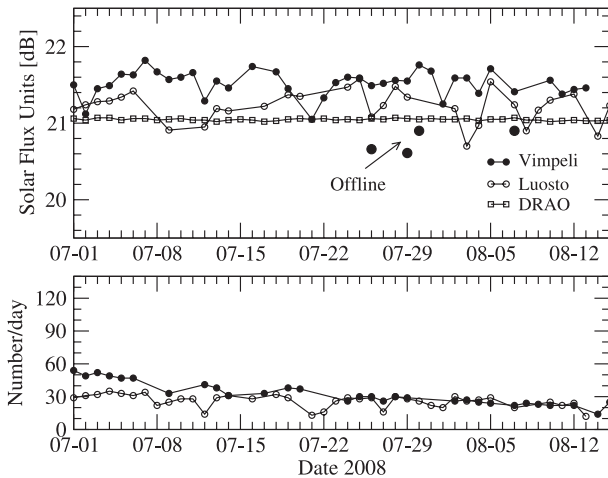


FIG. 3. Daily analysis of the sun signatures observed by the weather radars in Vimpeli (filled circles) and Luosto (open circles) from 1 Jul to 13 Aug 2008. For reference, the observations from DRAO are plotted as well. The results from the offline sun-pointing experiments in Vimpeli are also plotted.

only uses the five lowest elevations, which are repeated every 5 min, whereas KNMI uses all elevations, except the lowest two, amounting to 12. There are also differences in the processing and sensitivity of the weather radars. Furthermore, missing data resulting from precipitation occur more often for FMI, because it may happen that the analyzed (low elevation) beams are not reaching above the rain. Note that the sun flux data from these radars (almost 500 km apart) are less correlated than those from the KNMI pair (100 km apart) shown in Fig. 2. This correlation is attributed to residuals of weather signals. When the daily solar flux data from the Vimpeli radar are referenced against those from the

Luosto radar, a small bias of +0.26 dB and a standard deviation of 0.20 dB are found.

The sun flux observed by the weather radar in Vimpeli is somewhat above the DRAO reference (+0.47 dB), and that observed by the Luosto radar is very close to the reference (+0.16 dB). The standard deviations of the daily ratios for Vimpeli and Luosto with respect to DRAO are 0.16 and 0.20 dB, respectively, during this summer period. Comparing Figs. 2 and 3 reveals a difference of about 1 dB between the receiver sensitivities of the KNMI and FMI weather radars, which may show up in the European weather radar composite (Holleman et al. 2008). The low standard deviations found for both the KNMI and FMI radars demonstrate the stability of the sun-based monitoring and the radar receiving chains.

b. Offline sun tracking

On 22 January 2008, the operational scanning of the weather radar in De Bilt was interrupted and offline sun tracking was performed. The sun tracking with the radar started before sunrise (0740 UTC) and ended after sunset (1600 UTC). The maximum elevation of the sun on this winter day was about 18.3° . During sunrise and sunset, the solar power received by the weather radar was recorded at approximately every degree in elevation. The results are plotted in Fig. 4 (left). The radar was running in long-pulse mode (0.6-MHz bandwidth) during sunrise and running in short-pulse mode (1.5-MHz bandwidth) during sunset. The observed difference in received sun power between long- and short-pulse modes is about 4 dB, which can be attributed fully to the ratio of the bandwidths (see Table 1). At low elevations, the received solar power decreases rapidly (i.e., about 2 dB

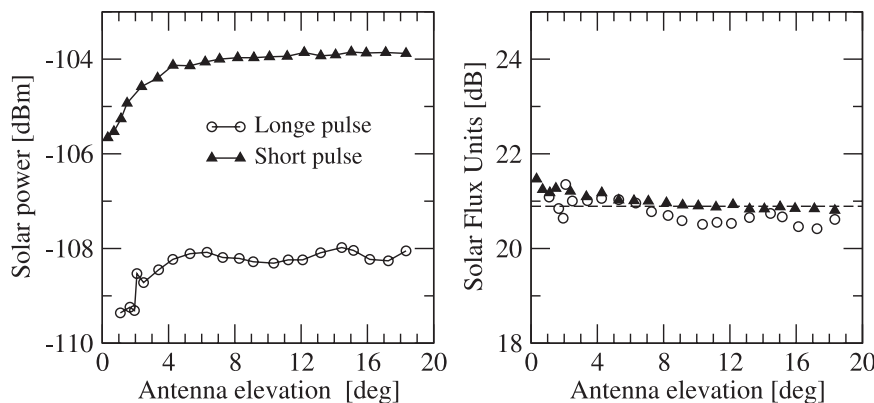


FIG. 4. Analysis of the offline sun measurements at the De Bilt radar on 22 Jan 2008. (left) The observed solar power during the morning ascent with receiver in long-pulse mode and the afternoon descent with receiver in short-pulse mode are shown. (right) The observed power converted to solar flux is shown.

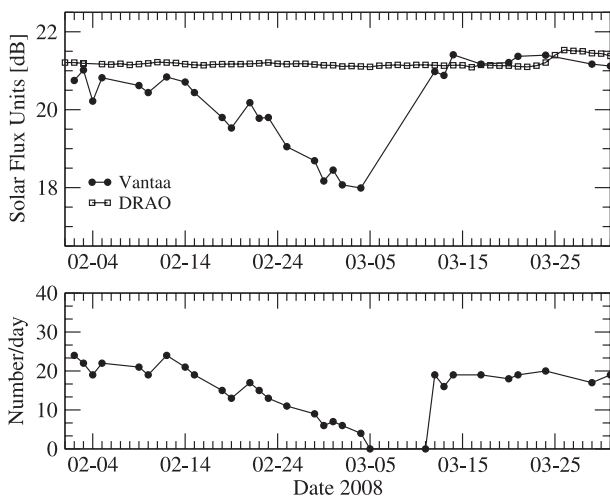


FIG. 5. Daily analysis of the sun signatures observed by the weather radar in Vantaa and the DRAO reference from 1 Feb to 31 Mar 2008. (top) The observed solar flux and (bottom) the number of analyzed sun signatures per day are shown.

in 4°) in both modes. This decrease is caused by the atmospheric gaseous attenuation.

Using Eqs. (4) and (15), the observed solar power from the tracking experiment has been converted to solar flux. Note that, for the data from the tracking experiment, no correction for scanning losses ($\Delta_a = 0$) and no model fit ($P_0 \equiv P_s$) are needed, because the antenna is optimally pointing at the sun. The resulting solar flux values are shown in Fig. 4 (right). It is evident that the differences between long- and short-pulse modes and the elevation dependence have been removed almost completely. This supports the validity of the gaseous attenuation model given by Eq. (2). The mean solar flux for the combined short- and long-pulse data is 20.89 ± 0.25 dB (in sfu). This value is plotted together with the online data in Fig. 2; considering the error bars, the agreement is really good.

Offline measurements were performed at the Vimpeli radar as well. Measurements were done on 25, 28, and 29 July and 6 August 2008, all close to noon. Measurements in the direction of the sun and in another direction (background) were differenced to get an estimate of the solar power. The power was converted to solar flux, and these flux values are plotted together with the online data in Fig. 3. The agreement with the online sun flux data and with the DRAO values is good.

5. Examples

a. Failing of harmonic filter

Figure 5 shows an example of how a gradual failure of radar components is seen in the daily sun flux data. The

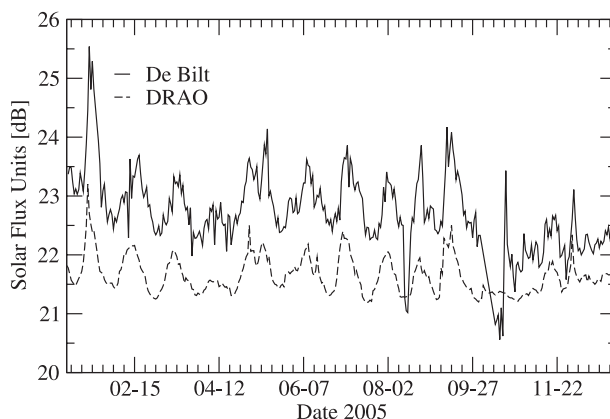


FIG. 6. Daily solar flux as observed by the weather radar in De Bilt and the DRAO reference over 2005. The solar rotation with a period of about 30 days can be seen clearly.

solar power is seen to diminish starting about 20 February 2008, and the number of sun hits also drops. The decrease in the power soon gets faster; on 4 March, the recorded power is about 4 dB lower than normal and the number of hits is down by a factor of 5. At this point, the cause of the power loss was revealed to be degradation of the harmonic filter in the waveguide. After replacement of the filter, the sun power and the number of sun signatures returned to typical values.

b. Solar monitoring during active episode

The daily solar flux over 2005 as observed by the weather radar in De Bilt and DRAO is shown in Fig. 6. A clear oscillation of about 1 dB is seen in both observations, and it is almost perfectly correlated. The oscillation has a period of about 1 month and it is due to the rotation of the sun (Tapping 2001). During active periods, the sun contains a number of active regions (e.g., sunspots), which emit radio-frequency radiation. Because of the solar rotation, the number of active regions as seen from the earth varies; thus, the solar flux received by the radar changes. The activity of the sun has roughly a 10–13-yr cycle. The solar rotation can only be observed in the radio-frequency flux during active episodes. The receiving bias and standard deviation of De Bilt with respect to DRAO are +1.06 and 0.44 dB, respectively, during this active episode. The higher standard deviation with respect to the results in Fig. 2 is attributed to the increased activity of the sun.

6. Conclusions

In this paper, we present an extension of the method for determining the weather radar antenna pointing at low elevations using sun signals (Huuskonen and Holleman

2007) to monitoring of the receiving chain. The sun monitoring method is entirely based on analysis of the polar volume data produced during operational scanning of the weather radars, and it is suited for routine application. The offline use of the sun for alignment of the radar antenna and checking the effective antenna system gain is rather common and the conversion of the “reflectivity” from the sun to the received solar flux is well known. When analyzing sun signals in polar volume data from operational scans, additional corrections are required for the refraction and atmospheric attenuation of the solar radiation at low elevations and for attenuation resulting from the scanning antenna.

The solar flux from the online analysis has been compared to the flux from offline sun tracking experiments at two weather radars. The online and offline sun fluxes agree within 0.1 dB for the radar in De Bilt and within 0.7 dB for the one in Vimpeli. Furthermore, the retrieved sun flux is compared with the data from the Dominion Radio Astrophysical Observatory (DRAO). Against DRAO, sun flux biases between -0.93 and $+0.47$ dB are found for the Dutch and Finnish radars. The low standard deviations between 0.14 and 0.20 dB demonstrate the stability of the sun-based monitoring and the radar receiving chains.

As an example of a successful application of sun monitoring, a case of a failing harmonic filter in the Finnish radar network has been discussed. In the daily solar flux over 2005 from the weather radar in De Bilt, the monthly solar rotation can be clearly seen. This shows that, even during active solar episodes, operational weather radars can accurately monitor the radio-frequency signal of the sun.

Results from a daily analysis of the sun signals in radar data can be used for monitoring the alignment of the radar antenna and the stability of the radar receiving chain. In a national or international network of operational weather radars, differences in the sensitivity of the receiving chain, including the antenna gain and the receiver, can be brought to light. By comparison with the observations from a sun flux monitoring station, even the calibration of the receiving chain can be checked. The method presented in this paper has great potential for routine monitoring of the weather radars in national or international networks [e.g., the European network of the Operational Programme for the Exchange of Weather Radar Information (OPERA); Holleman et al. 2008].

Acknowledgments. Peter Gözl from SELEX-SI is gratefully acknowledged for useful discussions and feedback. The valuable comments from the anonymous reviewers are appreciated.

REFERENCES

- Andersson, T., 2000: Using the sun to check some weather radar parameters. Swedish Meteorological Hydrological Institute (SMHI) Rep. RMK 93, 30 pp.
- Beekhuis, H., and I. Holleman, 2008: From pulse to product: Highlights of the digital-IF upgrade of the Dutch national radar network. *Proc. Fifth European Conf. of Radar Meteorology and Hydrology*, Helsinki, Finland, ERAD, P9.11.
- Darlington, T., M. Kitchen, J. Sugier, and J. de Rohan-Truba, 2003: Automated real-time monitoring of radar sensitivity and antenna pointing accuracy. *Proc. 31st Conf. on Radar Meteorology*, Seattle, WA, Amer. Meteor. Soc., 538–541.
- Doviak, R. J., and D. S. Zrnić, 1993: *Doppler Radar and Weather Observations*. 2nd ed. Academic Press, 562 pp.
- Holleman, I., and H. Beekhuis, 2003: Analysis and correction of dual-PRF velocity data. *J. Atmos. Oceanic Technol.*, **20**, 443–453.
- , and —, 2004: Weather radar monitoring using the sun. Royal Netherlands Meteorological Institute (KNMI) Tech. Rep. TR-272, 40 pp.
- , L. Delobbe, and A. Zgonc, 2008: Update on the European Weather Radar Network (OPERA). *Proc. Fifth European Conf. of Radar Meteorology and Hydrology*, Helsinki, Finland, ERAD, 3.3.
- Huuskonen, A., and I. Holleman, 2007: Determining weather radar antenna pointing using signals detected from the sun at low antenna elevations. *J. Atmos. Oceanic Technol.*, **24**, 476–483.
- Press, W. H., S. A. Teukolsky, W. T. Vetterling, and B. P. Flannery, 1992: *Numerical Recipes in C: The Art of Scientific Computing*. 2nd ed. Cambridge University Press, 994 pp.
- Probert-Jones, J. R., 1962: The radar equation in meteorology. *Quart. J. Roy. Meteor. Soc.*, **88**, 486–495.
- Rinehart, R. E., 2004: *Radar for Meteorologists*. 4th ed. Rinehart, 482 pp.
- Salonen, K., G. Haase, H. Järvinen, A. Huuskonen, and L. Neuvonen, 2008: Towards the operational use of Doppler radar radial wind observations in HIRLAM at FMI. *Proc. Fifth European Conf. of Radar Meteorology and Hydrology*, Helsinki, Finland, ERAD, 11.8.
- Sirmans, D., D. Zrnić, and B. Bumgarner, 1976: Extension of maximum unambiguous Doppler velocity by use of two sampling rates. *Proc. 17th Conf. on Radar Meteorology*, Seattle, WA, Amer. Meteor. Soc., 23–28.
- Tapping, K., 2001: Antenna calibration using the 10.7 cm solar flux. Preprints, *Workshop on Radar Calibration*, Albuquerque, NM, Amer. Meteor. Soc. [Available online at http://www.k5so.com/RadCal_Paper.pdf.]
- Whiton, R. C., P. L. Smith, and A. C. Harbuck, 1976: Calibration of weather radar systems using the sun as a radio source. *Proc. 17th Conf. on Radar Meteorology*, Seattle, WA, Amer. Meteor. Soc., 60–65.